

# novH: Differential Expression in Developing Kidney and Wilms' Tumors

Gaëlle Chevalier,\* Herman Yeger,<sup>†</sup>  
Cécile Martinerie,\* Maryvonne Laurent,\*  
Jennifer Alami,<sup>†</sup> Paul N. Schofield,<sup>‡</sup> and  
Bernard Perbal\*<sup>§</sup>

*From the Laboratoire d'Oncologie Virale et Moléculaire,\* INSERM U142 Hôpital Saint-Antoine, Paris, France; the Department of Pediatric Laboratory Medicine,<sup>†</sup> Hospital for Sick Children and University of Toronto, Toronto, Canada; the Laboratory of Stem Cell Biology,<sup>‡</sup> Department of Anatomy, University of Cambridge, Cambridge, United Kingdom; and the UFR de Biochimie,<sup>§</sup> Université Paris 7-D. Diderot, Paris, France*

**We previously established that the expression of the human nov gene (novH) was altered in Wilms' tumors and that levels of novH and WT1 mRNA were inversely correlated in individual Wilms' tumors. Insofar as novH has been shown to be a target for WT1 regulation, novH might play an important role during normal nephrogenesis and in the development of Wilms' tumors. We now show that during normal nephrogenesis novH protein is tightly associated with differentiation of glomerular podocytes. NovH expression is not restricted to renal differentiation but is also detected in endothelium and neural tissue of the kidney. Our results establish that alteration of novH expression in sporadic and heritable Wilms' tumors is associated with dysregulated expression of both novH mRNA and protein. In general, the highest novH expression was noted in the Wilms' tumor, genitourinary anomalies, aniridia, and mental retardation (WAGR)-associated Wilms' tumors. Expression in the Denys-Drash syndrome (DDS)-associated Wilms' tumors fell within the variable spectrum observed in sporadic Wilms' tumor cases. As in developing kidney podocytes, novH protein was also prominent in the abnormal hypoplastic podocytes from DDS cases and in kidney podocytes adjoining Wilms' tumors. In Wilms' tumors exhibiting heterotypic differentiation, novH protein was expressed at high levels in tumor-derived striated muscle and at lower levels in tumor-derived cartilage. These observations taken together indicate that novH may represent both a marker of podocytic differentiation in kidney and a marker of heterotypic mesenchymal differentiation in Wilms' tumors. In addition, absence or very low levels of WT1 are correlated with higher novH expression, and its variable expression in cases with mutant WT1 (sporadic and DDS) suggests that the**

**potential activation and repression transcriptional functions possessed by WT1 are likely dependent on the specific mutation incurred. (*Am J Pathol* 1998, 152:1563-1575)**

Wilms' tumor is a kidney cancer that affects approximately 1 in 10,000 children usually between 3 and 6 years of age.<sup>1-3</sup> The majority of Wilms' tumors occur sporadically (99%) and are unilateral (93%). However, there are heritable Wilms' tumors (1%), which are diagnosed earlier (at 2 to 3 years of age) and are usually bilateral.<sup>1</sup> These tumors can occur in association with several other pathologies, defining the Denys-Drash (DDS; Wilms' tumor, male pseudohermaphroditism, and renal failure), WAGR (Wilms' tumor, genitourinary anomalies, aniridia, and mental retardation), and Beckwith-Wiedemann (gigantism and visceral hypertrophy) syndromes.

In the classical triphasic Wilms' tumors, tumor blastema resembles undifferentiated metanephric mesenchyme and can also give rise to dysplastic tubules and pseudoglomeruli in these tumors, reflecting an abnormal pattern of kidney-specific differentiation. Variants of Wilms' tumors exhibit different proportions of each of the blastemal, stromal, and epithelial components ranging from infrequent to abundant. In a significant proportion of cases, Wilms' tumors also display nonrenal heterotypic differentiated tissues, such as muscle, observed most frequently, but also cartilage and bone, all resulting from aberrant mesenchymal differentiation.<sup>4</sup>

Several genetic alterations, involving loss of heterozygosity of the 11p13, 11p15, 11q, 7p, and 16q chromosomal regions, have been associated with Wilms' tumor development and progression.<sup>5-13</sup> As the majority of Wilms' tumors carry few alterations in these regions, the

---

Supported by grants to B. Perbal from Association Pour la Recherche Contre le Cancer, Ligue Nationale Contre le Cancer (Comités National, du Loir et Cher et de l'Indre), Fondation Pour la Recherche Médicale, and Association Française contre les Myopathies and to H. Yeger from funds provided by the Canadian Cancer Society to the National Cancer Institute, Canada. Work in the laboratory of P.N. Schofield was funded by the National Kidney Research Fund. Gaëlle Chevalier was the recipient of a fellowship from British Council and was supported by the French Ministère de la Recherche et de la Technologie.

Accepted for publication March 13, 1998.

Address reprint requests to Pr. Bernard PERBAL, UFR de Biochimie, Tour 42, Université Paris 7- D. Diderot, 2 Place Jussieu, 75005 Paris, France. E-mail: bernard.perbal@wanadoo.fr.

existence of additional WT loci has been postulated. Despite the considerable amount of information obtained regarding the biological and biochemical properties of the WT1 gene, which resides at 11p13 (for reviews see Refs. 14–16), little is known about other genes that may be responsible for initiation and/or maintenance of the Wilms' tumor state.

To identify such genes we have initiated a study of avian myeloblastosis-associated virus (MAV1N)-induced nephroblastomas, which constitute a unique animal model of Wilms' tumors.<sup>17</sup> Analysis of MAV-induced nephroblastomas led us to the discovery of the nov (nephroblastoma overexpressed) gene, the expression of which was increased in all nephroblastomas.<sup>18</sup> The nov gene shared extended nucleotide sequence similarities with two groups of immediate-early genes (ctgf/fisp12 and cyr61/cef10) encoding positive cell growth regulators acting cooperatively with growth factors.<sup>18–27</sup> A comparative analysis of the CTGF/FISP12, CYR61/CEF10, and NOV primary structures established that these proteins contain 38 conserved cysteine residues and four structural motifs: 1) an IGFBP module, homologous to the insulin-like growth factor (IGF)-binding domain of previously described IGF-binding protein (IGFBP), 2) a VWC module likely to be involved in oligomerization and represented in von Willebrand factor, 3) a TSP1 module, represented in thrombospondin, and thought to be involved in the interaction with extracellular matrix molecules, and 4) a carboxyl-proximal motif proposed to represent a dimerization domain.<sup>19</sup> Although the functionality of these domains remain to be experimentally established, it is tempting to propose that their conservation is related to the biological function(s) of these proteins.

Despite their highly conserved organization, the immediate-early ctgf/fisp12 and cyr61/cef10 genes are subjected to different regulatory signals and encode positive regulators of cell growth with distinct biochemical properties. Both CTGF and CYR61 are secreted. They exhibit mitogenic and chemotactic activities.<sup>20,21,26</sup> Whereas CTGF is released in the cell culture medium, the CYR61 protein remains associated with the extracellular matrix and cell surface.<sup>20,25</sup> Recent results have established that CTGF is a downstream target of transforming growth factor (TGF)- $\beta$  signaling pathway.<sup>21</sup>

Early experiments established that the overexpression of nov in normal embryonic fibroblasts was interfering with their growth *in vitro*.<sup>18</sup> Moreover, the expression of nov was associated with cell quiescence and was down-regulated on induction of cell proliferation after serum or tetradecanoyl phorbol acetate induction and oncogenic transformation.<sup>28</sup> These distinctive features raised the possibility that nov is a negative regulator of cell growth and could have an antagonist effect compared with the CTGF and/or CYR61 stimulatory effects.<sup>17</sup>

We have previously established that expression of the human nov gene (novH) was down-regulated by the WT1 proteins in *ex vivo* assays, indicating that novH was a potential target of WT1.<sup>29</sup> In addition, we have demonstrated that expression of the nov gene was also altered

in Wilms' tumors and that levels of novH and WT1 mRNA were inversely correlated in these tumors.<sup>30</sup> The variations in the novH mRNA level detected in different tumors suggested that elevated novH expression may be related to a particular histological subgroup of Wilms' tumors.<sup>30</sup> All together, these results lead to the hypothesis that novH might be involved in nephrogenesis and associated with development of Wilms' tumors.

As a first step in establishing the biological function(s) of nov and its involvement in nephrogenesis, we have further characterized the novH protein and performed *in situ* hybridization and immunohistochemistry on normal human fetal and adult kidney sections and on different Wilms' tumors samples representative of sporadic, WAGR, and DDS cases.

We now provide evidence that, during normal nephrogenesis, novH protein accumulates in glomerular podocytes and that increased novH protein in Wilms' tumor is correlated with heterotypic differentiation, in particular, muscle differentiation. Thus, novH expression may serve as a marker of Wilms' tumor heterotypic differentiation.

## Materials and Methods

### Tissue Samples

Human embryos of 10 to 22 weeks gestational age were obtained from the Medical Research Council (MRC) Tissue Bank after therapeutic termination of pregnancy by mechanical aspiration or prostaglandin treatment. Embryonic stage was determined by crown/rump and foot length together with estimated time of last menstruation. All embryos were judged to be normal by morphological criteria. After washing in cold phosphate buffered saline solution, embryos were fixed in ice cold fresh phosphate-buffered 4% w/v paraformaldehyde solution within 2 minutes of delivery or in 10% neutral buffered formalin according to standard protocol for histopathology. In a few cases, tissues were also fixed in Histochoice tissue fixative (Amresco, Solo, OH) for comparison.

A series of 12 Wilms' tumors, including sporadic and WAGR cases (GOS 543, GOS 157, and BA tumors), as well as 3 cases of DDS-associated kidneys were obtained from the Department of Pathology at the Hospital for Sick Children, London, UK; 40 Wilms' tumors, including a case of desmoplastic round-cell tumor from the Hospital for Sick Children, Toronto, Canada; and 3 cases of Denys-Drash tumors from Dr. Jaubert, Hôpital Necker, Paris, France. Altogether, the cases studied represented both pre- and post-chemotherapy resected tumors. A number of these cases have been previously studied with respect to WT1 mutations, chromosome 11 loss of heterozygosity, and expression and involvement of p53.<sup>31,32</sup> A case of Wilms' tumor showing a prominent area of nephroblastomatosis, Wilms' 2007, was kindly provided by Dr. El-Naggar, MD Anderson Center, Houston, TX. Most tumors cases were fixed in formalin, a few in Bouin's fixative, and all were paraffin embedded.

## Expression Vectors

The 1970-bp novH cDNA<sup>30</sup> (EMBL accession number X96584) was subcloned in both sense and antisense orientations in the pCB6 expression vector<sup>33</sup> containing the cytomegalovirus major immediate-early promoter and the SV40 polyadenylation signal to generate, respectively, pCMV-novH (S) and pCMV-novH (AS) and in the baculovirus transfer vector pVL1392 (PharMingen, San Diego, CA) to generate pVL82 (sense) and pVL84 (antisense) vectors.

## Cell Cultures and Transfections

The Madin Darby canine kidney (MDCK) cell line,<sup>34</sup> kindly provided by Dr. Jouanneau, Institut Curie, Paris, France, was grown in Dulbecco's modified Eagle's medium (DMEM; Gibco/BRL, Gaithersburg, MD) supplemented with 10% fetal calf serum.

MDCK cells were stably transfected with pCMV-novH(S) or pCMV-novH(AS) subclone DNA (6  $\mu$ g) in the presence of Lipofectamine (Gibco/BRL). After neomycin selection, individual clones were picked and expanded. Total cell proteins were prepared from confluent stably transfected MDCK cells in RIPA buffer as previously described.<sup>35</sup>

*Spodoptera frugiperda* (SF9) insect cells were grown in TC100 medium (Gibco/BRL) supplemented with 10% fetal calf serum. Recombinant pVL82 and pVL84 viruses production was achieved using the Baculogold transfection system (PharMingen). Culture media of transfected cells were collected after 4 days of culture and used to infect fresh SF9 cells for virus production. Serum-free conditioned medium was collected 48 hours after infection of SF9 cells with pVL82 or pVL84 recombinant viruses. Lyophilized conditioned medium and infected SF9 cells were, respectively, resuspended and lysed in the buffer recommended for protein analysis by the manufacturer (PharMingen). Protein concentrations were estimated by Lowry method.

## Antibody Preparation

A peptide specific to the carboxyl-terminal region of novH (amino acids 339 to 357, KNNEAFLQELELKTRGKM) was coupled to activated keyhole limpet hemocyanin<sup>36</sup> and used to generate a rabbit polyclonal antibody (K19M).

## Metabolic Cell Labeling and Immunoprecipitation Analysis

MDCK cells transfected with pCMV-novH(S) (subclone 54.14) or pCMV-novH(AS) (subclone 51.2) were preincubated in a methionine/cysteine-free modified Eagle's medium (MEM; Gibco/BRL) medium supplemented with 0.5% dialyzed calf serum for 60 minutes. Newly synthesized proteins were labeled by adding 100  $\mu$ Ci/ml of a [<sup>35</sup>S]methionine/cysteine mixture (specific activity, 1000 Ci/mmol; Amersham, Arlington Heights, IL). After a 2-hour

incubation, the cells were lysed in RIPA buffer as previously described.<sup>35</sup>

Labeled conditioned medium was concentrated using Centricon C30 (Amicon, Beverly, MA). Immunoprecipitation was performed essentially as previously described. [<sup>35</sup>S]-Labeled lysates or concentrated conditioned media were first precleared for 60 minutes with 20  $\mu$ l of protein A-Sepharose slurry (Pharmacia, Uppsala, Sweden; 50% in RIPA buffer containing 2% bovine serum albumin) and incubated for an additional 60 minutes at 4°C with K19M antiserum at a dilution of 1:150 followed by a 60-minute incubation at 4°C with 30  $\mu$ l of protein A-Sepharose slurry.

For pulse-chase experiments, subclone 54.14 cells were labeled for 45 minutes with 100  $\mu$ Ci/ml of the [<sup>35</sup>S]methionine/cysteine mixture. After the pulse label, cells were washed twice with PBS and then incubated with 5 ml of complete medium (DMEM supplemented with 0.5% fetal calf serum). Both cells and medium were harvested at 0 and 30 minutes and 1.5, 2.5, 4.5, 6.5, and 18 hours of chase time and processed as described above for novH analysis by immunoprecipitation.

## Western Blot Immunoassay

Protein samples were electrophoresed on a SDS/10% polyacrylamide gel and electroblotted onto polyvinylidene difluoride filters (Immobilon P, Millipore, Bedford, MA). Blots were incubated with anti-novH polyclonal serum K19M at a dilution of 1:500 for 1 hour at 37°C. Immunocomplexes were visualized using enhanced chemiluminescence as described by the manufacturers (Dupont NEN, Boston, MA, and Boehringer Mannheim, Indianapolis, IN).<sup>32</sup>

## Heparin-Binding Assays

Confluent MDCK transfected cells were cultured for 24 hours in serum-free medium. Both cell extracts or conditioned media were collected and incubated overnight at 4°C with 200  $\mu$ l of a 50% slurry of heparin-Sepharose beads (Pharmacia). After washing with 5 ml of PBS, proteins were eluted with PBS containing 0.4 mol/L NaCl. The presence of novH protein was analyzed by Western blotting.

## In Situ Hybridization

For *in situ* hybridization, the pBX1.5 plasmid containing the 1.5-kb *Bgl*II-*Xho*I novH genomic fragment<sup>30</sup> was digested by *Xba*I or *Xho*I. The 3.5-kb *Xba*I (antisense) or 4.4-kb *Xho*I (sense) digestion fragments were gel fractionated and eluted. The 3' untranslated novH sequences were transcribed from the T7 (antisense) or T3 (sense) promoters in the presence of 0.35 mmol/L digoxigenin-11-UTP (Boehringer Mannheim) to generate a 620-nucleotide antisense digoxigenin novH riboprobe (*Xb*3.5) or a 1500-nucleotide sense digoxigenin riboprobe. Labeled RNAs were separated from unincorporated nucleotide triphosphates by precipitation with 0.4 mol/L LiCl in eth-

anol and quantified by spot tests using chemiluminescence detection. The full-length sense riboprobe was further reduced into smaller fragments by alkaline hydrolysis as previously described.<sup>37</sup> *In situ* hybridizations were performed on 5- $\mu$ m, formalin-fixed, paraffin-embedded sections as previously described,<sup>38,39</sup> using digoxigenin-labeled novH riboprobe Xb3.5 diluted to a final concentration of 0.8  $\mu$ g/ml in hybridization buffer. Negative controls were performed using sense riboprobe.

### Immunohistochemistry

Immunohistochemistry experiments were performed on 5- $\mu$ m, formalin-fixed, paraffin-embedded sections, essentially as previously described, using the K19M antibody at 1:250.<sup>38</sup> The peroxidase enzyme reaction was developed for 5 to 20 minutes in diaminobenzidine solution (Research Genetics, Huntsville, AL), and sections were counterstained with hematoxylin-ammonia bluing and mounted with Permount after dehydration step. Controls consisted of incubation leaving out the primary antibody or preincubation of the K19M antibody with 10  $\mu$ g/ml specific peptide. In both controls, no specific staining was observed.

## Results

### NovH Is a Secreted Protein

Baculovirus-infected SF9 cells were used to characterize the novH protein by Western blotting. A 44-kD novH protein was detected by K19M antibody in conditioned medium whereas two novH isoforms of 45 and 43 kD were detected in cellular extracts from pVL82-infected cells (Figure 1A, lanes 1 and 2). Competition with the specific 19-amino-acid peptide used to generate the K19M antibody completely abolished the novH protein recognition, and the K19M antibody did not detect novH protein in control SF9 cells infected with pVL84 recombinant baculovirus (Figure 1A, lanes 3–8). These results indicated that the K19M antibody specifically recognized the novH protein and demonstrated that the novH protein was secreted by pVL82-infected SF9 cells.

Although endogenous nov mRNA was detected in nontransfected MDCK cells (data not shown), the K19M antibody did not recognize dog nov protein by Western blotting in these cells, likely due to sequence differences in the carboxyl-terminal end. MDCK cells were therefore stably transfected with pCMV-novH(S) to establish whether the novH protein could also be secreted by mammalian cells. Both transfected cell extracts and conditioned medium contained high levels of a 48-kD novH protein as revealed by immunoprecipitation and Western blotting (Figure 1, B and C). Cellular extracts contained an additional 44-kD novH protein isoform not found in the culture medium (Figure 1B, lane 2). As in nontransfected cells, the K19M antibody did not detect novH protein in control pCMV-novH(AS)-transfected MDCK cells (Figure 1B).

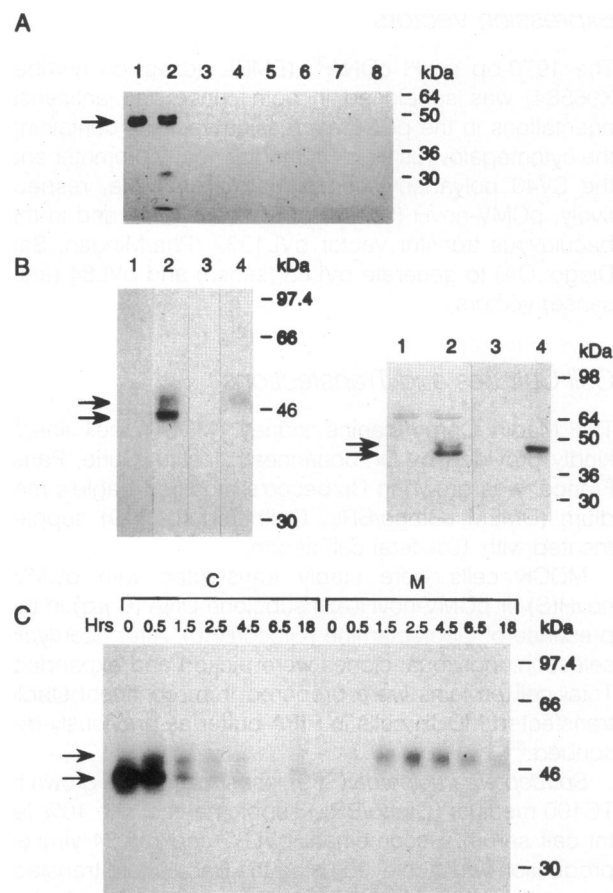


**Figure 1.** Secretion of novH protein in insect and mammalian cells. **A:** Secretion of novH protein by baculovirus-infected SF9 cells. SF9 cells were infected with pVL82 (novS) (lanes 1, 2, 5, and 6) or pVL84 (novAS) (lanes 3, 4, 7, and 8) baculoviral vectors as described in Materials and Methods. Culture media (lanes 1, 3, 5, and 7) or cell extracts (20  $\mu$ g of proteins) (lanes 2, 4, 6, and 8) were analyzed by Western blotting using the K19M antibody at a dilution of 1:500 (lanes 1 to 4). Controls were performed by preincubating the K19M antibody with 10  $\mu$ g/ml of the 19-amino-acid novH-specific peptide (K19M peptide; lanes 5 to 8). Arrows indicate the position of novH proteins. Molecular weight of size markers is indicated in kilodaltons. **B:** Secretion of novH protein by MDCK-transfected cells. MDCK cells were transfected by either pCMV-novH(AS) or pCMV-novH(S) DNA as described in Materials and Methods. Individual clones selected with neomycin were screened for novH expression by Western blotting analysis with the K19M antibody. A positive clone (54.14; lanes 2 and 4) and negative clone (51.2; lanes 1 and 3) were selected for further analysis. **Left panel:** [<sup>35</sup>S]Methionine-cysteine-labeled cell extracts (5  $\times$  10<sup>6</sup> cpm as determined by TCA precipitation; lanes 1 and 2) or conditioned medium (lanes 3 and 4) were immunoprecipitated with the K19M antibody diluted at 1:150. **Right panel:** Cell extracts (70  $\mu$ g of proteins, representing 1/20 of cells from a 6-cm dish; lanes 1 and 2) or conditioned medium (20  $\mu$ l, representing 1/200 of medium from the same 6-cm dish; lanes 3 and 4) were analyzed by Western blotting using the K19M antibody diluted at 1:500. **C:** Determination of the half-life of the novH protein. Cell extracts (C) or conditioned medium (M) from MDCK subclone 54.14 cells, pulse-labeled as described in Materials and Methods, were immunoprecipitated with the K19M antibody at a dilution of 1:200 after 0, 0.5, 1.5, 2.5, 4.5, 6.5, and 18 hours of chase time.

Comparison of intra- and extracellular protein amounts after 48 hours of culture also indicated that approximately 80% of novH produced by these cells was found in the medium, suggesting that the extracellular novH protein was stable (Figure 1B).

To determine the kinetics of novH protein synthesis and secretion, confluent pCMV-novH(S)-transfected MDCK cells were pulse-labeled as described in Materials

and Methods and further incubated in unlabeled medium for various durations. At each of the time points in the chase experiment, both cell extracts and medium were harvested and immunoprecipitated with the K19M antibody. As shown in Figure 1C, before chase, the majority of the novH protein resided intracellularly and was of the 44-kD form. Newly synthesized novH protein increased in molecular weight after 30 minutes of chase and was first detectable in the extracellular medium after 1.5 hours of chase, indicating that the novH protein was rapidly synthesized and secreted. Analysis of the amount of novH protein using a Phosphorimager (Molecular Dynamics, Sunnyvale, CA) revealed that the apparent half-life of intracellular novH was approximately 1.5 hours, whereas novH has a half-life of greater than 18 hours in the medium. These observations indicated that the extracellular pool of novH protein was more stable than the intracellular pool. This result was consistent with the immunoblotting experiments showing that novH protein accumulated in the extracellular medium (Figure 1B). Furthermore, the apparent increase in molecular weight also suggested progressive post-translational modification of novH protein with an increase of ~4 kD.

Subcellular localization of novH protein in pCMV-novH(S)-transfected MDCK cells was determined by immunofluorescence (data not shown). Incubation of live cells with the K19M antibody resulted in labeling at the level of intercellular boundaries, whereas permeabilization of cells with Triton X-100 showed localization of novH both in cytoplasm and at the membrane level. These results were in agreement with our *in vitro* results, indicating that novH protein was present both intracellularly and extracellularly.

### NovH Is a Glycosylated Protein

As the predicted molecular weight of novH protein was 39 kD, detection of 44- and 48-kD novH proteins suggested that both intra- and extracellular forms undergo post-translational modifications. Inasmuch as two putative *N*-glycosylation sites were present at position 97 (NQTG) and 280 (NCTS) in the novH polypeptide sequence, experiments were designed to study whether tunicamycin could interfere with novH protein post-translational modifications. Addition of tunicamycin (1  $\mu$ g/ml) to the culture medium of pCMV-novH(S)-transfected cells resulted in the detection of an intracellular 39-kD novH protein (Figure 2A, lane 2), suggesting that the 44- and 48-kD novH isoforms resulted from differential post-translational glycosylations, and in the detection of extracellular novH protein(s) with slightly different molecular weight(s) than that of the intracellular 39-kD novH protein. As this extracellular protein migrated as a smear (Figure 2A, lane 5), it suggested that it was subject to degradation. The K19M antibody did not detect any intra- or extracellular protein in pCMV-novH(AS)-transfected cells (Figure 2A), either in the presence (lanes 4 and 8) or absence (lanes 3 and 7) of tunicamycin.

To our knowledge, no other protein of the nov family (CYR61, CEF10, and FISP12) but CTGF<sup>40</sup> has been re-

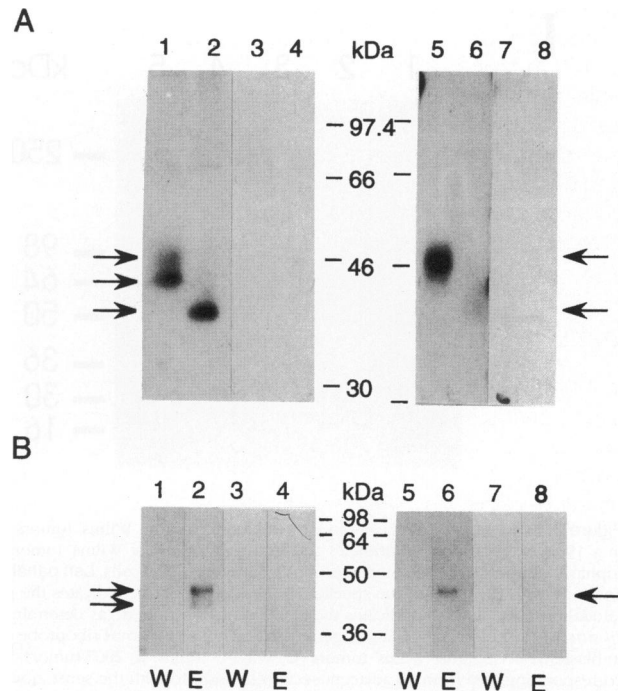


**Figure 2.** The novH protein is glycosylated and binds to heparin. **A:** MDCK subclone 54.14 (lanes 1, 2, 5, and 6) and subclone 51.2 (lanes 3, 4, 7, and 8) cells were preincubated during 18 hours in the absence or in the presence of the *N*-glycosylation inhibitor tunicamycin (1  $\mu$ g/ml) and further labeled for 2 hours as described in Materials and Methods in the absence (lanes 1, 3, 5, and 7) or in the presence (lanes 2, 4, 6, and 8) of the inhibitor. [<sup>35</sup>S]Methionine-cysteine-labeled cell extracts ( $5 \times 10^6$  cpm as determined by TCA precipitation; lanes 1 to 4) or conditioned medium (lanes 5 to 8) were immunoprecipitated with the K19M antibody at a dilution of 1:150. **Arrows** indicate the position of novH protein. Molecular weight of size markers is indicated in kilodaltons. **B:** Total proteins contained either in cell extracts (lanes 1 to 4) or conditioned medium (lanes 5 to 8) from MDCK subclones 54.14 (lanes 1, 2, 5, and 6) and 51.2 (lanes 3, 4, 7, and 8) were incubated with heparin-Sepharose beads, and elution was achieved at 0.55 mol/L NaCl. Analysis of wash (W) and elution (E) fractions was performed by Western blotting using the K19M antibody.

ported to be glycosylated. It is also interesting to point out that novH protein bound to heparin columns under conditions previously used to partially purify CYR61<sup>25</sup> (Figure 2B). However, novH was eluted at a salt molarity (0.55 mol/L) somewhat different from that used to elute CYR61 (Figure 2B). Thus, these observations are suggestive of novH-specific biochemical properties.

### novH Is Differentially Expressed in Human Fetal Kidney

The evidence that novH mRNA expression was detectable by RNase protection on human fetal kidney (data not shown), novH protein was secreted by kidney cells in culture, and altered expression was found in kidney-derived Wilms' tumors led us to use *in situ* hybridization and immunohistochemistry to examine novH expression in human fetal kidney. Twenty-week-old human fetal kidney was chosen because at this developmental stage well developed nephrons are present in the inner cortical region, whereas the outer cortical region still contains all stages of epithelial differentiation of the metanephrogenic mesenchyme.

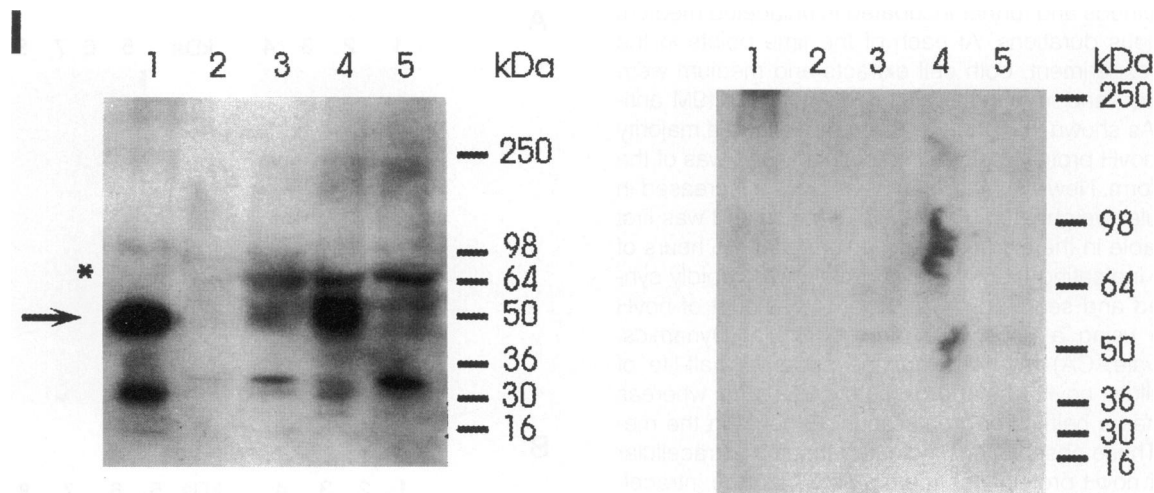


**Figure 3.** Expression of novH in human fetal kidney and in Wilms' tumors. I: Western blotting analysis (80  $\mu$ g of protein samples) of novH protein expression in a 19-week fetal kidney (lanes 2) and in three variants of Wilms' tumors (lanes 3, Wit-148, blastematos; lanes 4, Wit-141, heterotypic; lanes 5, Wit-146, triphasic). Lanes 1, culture media from pVL-82-infected SF9 cells. Left panel: K19M antibody at 1:500. Right panel: Control performed by preincubating the K19M antibody with 10  $\mu$ g/ml of the specific K19M peptide. Arrow indicates the position of the 44-kd novH protein. Molecular weight of size markers is indicated in kilodaltons. The asterisk indicates the position of HSA protein, as determined with a monoclonal anti-HSA antibody (Sigma, clone HSA-11; data not shown). II: *In situ* hybridization using a digoxigenin-labeled antisense novH riboprobe shows novH mRNA expression in developing epithelial structures of fetal kidney (A), in blastema of sporadic Wilms' tumors (C, Wit-149 tumor; E, 2007 tumor), and in Denys-Drash (F) and WAGR (H, GOS157 tumor) cases. Inset in C shows the corresponding area from an adjacent section hybridized with the sense novH riboprobe. Note elevated novH mRNA expression in tumor nodule (E, tn) but not in the adjacent nephroblastomatosis region (E, nb). B, D, G, and I: Immunohistochemistry study of novH protein expression using the K19M antibody. Note labeling of developing epithelial structures and podocytes of glomeruli of fetal kidney (B) and of blastema and pseudoglomeruli of sporadic (D, Wit-149 tumor), Denys-Drash (G), and WAGR (I, GOS157 tumor) Wilms' tumors. A and B: c, renal capsule; ct, collecting tubule; g, glomeruli; mm, metanephric mesenchyme; pct, proximal convoluted tubule; s, S-shaped body; v, epithelial vesicles. The arrow in B indicates presumptive podocytes of S-shaped body; arrowheads indicate podocytes of glomeruli. C to I: b, blastema; nb, nephroblastomatosis area; pg, pseudoglomeruli; s, stroma; tn, tumor nodule; v, vessel. Magnification  $\times 90$  (all except A, B, and E),  $\times 112.5$  (A and B)  $\times 14.4$  (E).

Hybridization of sections with the digoxigenin-labeled Xb3.5 antisense riboprobe detected appreciable novH mRNA in early epithelial vesicles, immature tubules, and S-shaped bodies (Figure 3A). Differentiated thin and ascending portions of loops of Henle (not present in this section) and collecting ducts were also positive. In contrast, novH mRNA was undetectable or minimal in undifferentiated mesenchymal cells, in stroma cells, in fully differentiated proximal convoluted tubules, and in well differentiated glomeruli (Figure 3A).

Moderate to high levels of novH protein were detected with the K19M antibody in metanephric mesenchyme, early epithelial vesicles, immature tubules, S-shaped bodies, podocytes of glomeruli, thin and ascending loops of Henle, and collecting ducts (Figure 3B and data not shown). Western blotting analysis showed varying levels of a 44-kd novH protein and a 30-kd novH-related polypeptide (Figure 3I). In addition to the novH-related proteins (44 and 30 kd), the K19M antibody cross-reacted with human serum albumin in Western blotting (Figure 3I, asterisk). Immunohistochemistry experiments using anti-HSA antibody on fetal kidney and Wilms' tumor sections showed no overlapping between novH and HSA sites of expression (data not shown). In differentiating structures, the level of novH mRNA detection was inversely correlated to the epithelial differentiation state, whereas the level of novH protein detected by K19M was found to increase with differentiation (Figure 3B). An identical pattern of novH mRNA and protein expression was observed in 10- to 22-week-old fetal kidney sections (data not shown), therefore indicating that the sites of

novH expression were not restricted to a particular developmental stage of the kidney within the 10- to 22-week fetal development period. In mature kidneys, the pattern of novH expression is maintained in glomeruli and collecting ducts (not shown). This likely indicates that regulation of novH expression is established early in development of the kidney.

### novH Expression in Wilms' Tumors

Northern blotting experiments previously established that novH expression was altered in Wilms' tumors.<sup>30</sup> To determine whether sites of novH mRNA expression and protein localization were different from those of normal fetal kidney, *in situ* hybridization, immunohistochemistry, and Western blot experiments were performed on a series of Wilms' tumors representing the spectrum of clinical presentations and associations.

As we had reported that novH promoter activity was down-regulated *ex vivo* by WT1 proteins, analyses for novH expression were performed on both blastematos and triphasic tumors with no reported alteration of the WT1 gene and in tumors bearing mutated forms of the WT1 gene. Wit-26 tumor contains a point mutation (deletion) in exon 10, leading to disruption of the normal open reading frame and resulting in a longer WT1 protein with an altered fourth zinc finger domain<sup>41</sup> whereas three WAGR syndrome-associated Wilms' tumors contain homozygous deletions of the WT1 gene. The GOS 543 tumor contained a 10-bp insertion into exon 7, resulting in



II

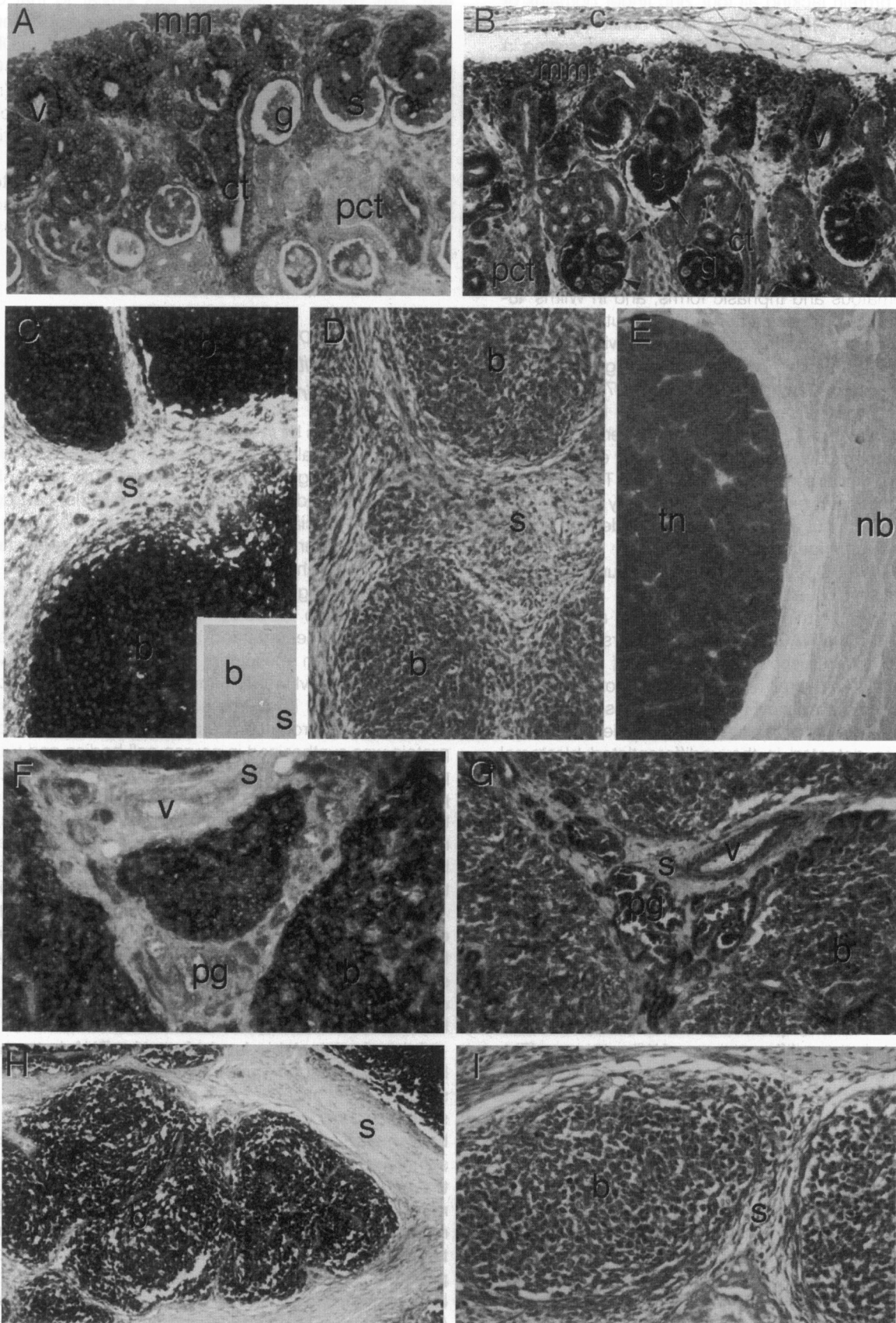


Figure 3. (Continued)

the generation of a stop codon and then production of a truncated protein lacking all four zinc finger domains of the WT1 protein.<sup>42</sup> The GOS 157 tumor contained a point mutation within exon 8 of the WT1 gene, also resulting in the generation of a stop codon and leading to a truncated protein missing the last three zinc finger domains.<sup>42</sup> The BA tumor contained a deletion in exon 10 (J. Cowell and P. Schofield, personal communication).

In contrast to normal blastema of fetal kidney, novH mRNA was generally expressed at moderate to high levels in the blastema of most of the Wilms' tumors. An example of the cellular expression pattern is seen in Figure 3C. Varying levels of novH mRNA were observed both in sporadic Wilms' tumors, including WT1-expressing blastematosus and triphasic forms, and in Wilms' tumors such as Wit-26 with a defined WT1 mutation (Figure 3C and data not shown). Hybridization with a control sense novH riboprobe revealed no staining (Figure 3C, inset). In a case of Wilms' tumor (Wilms' 2007) adjacent to a prominent area of nephroblastomatosis, novH mRNA was not detected in hyperplastic blastemal cells of nephroblastomatosis kidney but was highly expressed in blastema of the tumor nodule (Figure 3E). These results indicated that novH expression was not only deregulated in Wilms' tumors but was also likely dependent on acquisition of the tumorigenic state.

In a series of DDS-associated Wilms' tumors, where WT1 has been usually shown to exist in a dominant-negative mutant form<sup>43</sup> (Figure 3, F and G, and data not shown), and in the WAGR-associated tumors (Figure 3, H and I, and data not shown), expression of novH mRNA and protein were overall high but not proportional.

Although elevated novH mRNA expression was detected in blastema of all tumors, a low level of novH protein was detected in the undifferentiated blastemal cells of some of the WT1-positive blastematosus (Figure 3D) and triphasic tumors (not shown). This appeared to indicate that novH protein was not accumulated in these cells, possibly due to rapid degradation or to transport of novH to other sites. However, higher amounts of novH protein were detected in blastema of the Denys-Drash and WAGR-associated tumors (Figure 3, G and I), suggesting that in these tumors the mechanisms of either degradation or secretion of novH protein were likely to be different from those of tumors expressing unaltered WT1. Western blot analysis confirmed varying levels of expression of a 44-kd novH protein and a 30-kd novH-related polypeptide in three different types of Wilms' tumors (Figure 3I). The heterotypic Wit-141 Wilms' tumor contained more novH than homotypic tumors.

In all tumors, aberrant differentiation leading to the formation of dysplastic tubules and pseudoglomeruloids did not appear to interfere with either novH mRNA expression or novH protein localization (Figure 4, A and B, and data not shown). This was nicely demonstrated on a variant case of pseudoglomeruloid Wilms' tumor (Wit-75) where comparison of immunostaining for novH and an endothelial marker, QBEnd10 monoclonal antibody, which recognizes CD34 antigen specifically on vascular endothelium, demonstrated that novH protein was mainly localized in pseudoglomeruloids in association with

podocytes rather than with capillary endothelium (Figure 4C). This podocytic specificity was similar to that observed in normal glomeruli (Figure 3B), pseudoglomeruli within nephrogenic rests (Figure 4F), glomeruli from DDS cases, where glomerular sclerosis is present (Figure 4G), and in glomeruloid areas of nephroblastomatosis (not shown). Thus, intrinsically high expression of novH protein is associated with developing and maturing podocytes.

For the most part, the sites of novH mRNA and protein expression in the normal kidney adjacent to the tumors were identical to those observed in fetal kidney (compare Figure 1B and 4F).

### *novH Expression in Other Tissues and Relationship with Heterotypic Differentiation in Tumors*

Previous analysis by *in situ* hybridization and immunohistochemistry revealed that expression of chicken, mouse, and human nov genes was not restricted to kidney but was also detected in nervous system, muscle, cartilage, and bone<sup>16</sup> (Kocialkowski S, Chevalier G, Martinerie C, Kingdom J, Yeger H, Perbal B, Schofield PN, submitted, and our unpublished results).

As shown in Figure 5, A–D, novH expression in normal kidney was also detected in other differentiated cell types, such as neurons and both endothelium and surrounding smooth muscle of blood vessels. However, whereas both novH mRNA and protein were detected in endothelium and in neuron soma, only the protein was detected in neuronal processes, indicating that novH protein was synthesized in neuron cell bodies and transported along axonal processes. Similarly, elevated novH protein expression was detected in heterotypic differentiated tissues, which were characteristic of a significant number of Wilms' tumors. For example, a moderate to high level of novH protein was detected in foci of heterotypic cartilage (data not shown) and muscle differentiation.

An important observation was that high novH protein expression was not only found in cells with morphological features of striated muscle but could also be demonstrated in blastema with the phenotype of muscle by comparison of immunostaining of novH and desmin, a late muscle differentiation marker.

A barely detectable level of novH mRNA but a high level of novH protein was associated with desmin expression, both in highly differentiated muscle cells within the stroma (Figure 5, I and J, and data not shown) and in the blastemal component with a more mesenchymatous spindle cell morphology (Figure 5, G and H), indicated that novH expression coincided with heterotypic striated muscle differentiation. Moreover, in one case of a desmoplastic small round tumor, a tumor related to Wilms' tumor by virtue of the involvement of WT1,<sup>44–46</sup> novH protein immunostaining in blastemal cells extended to a larger population compared with desmin immunostaining (Figure 5, E and F), suggesting that novH protein might be an earlier marker than desmin for muscle differentiation.



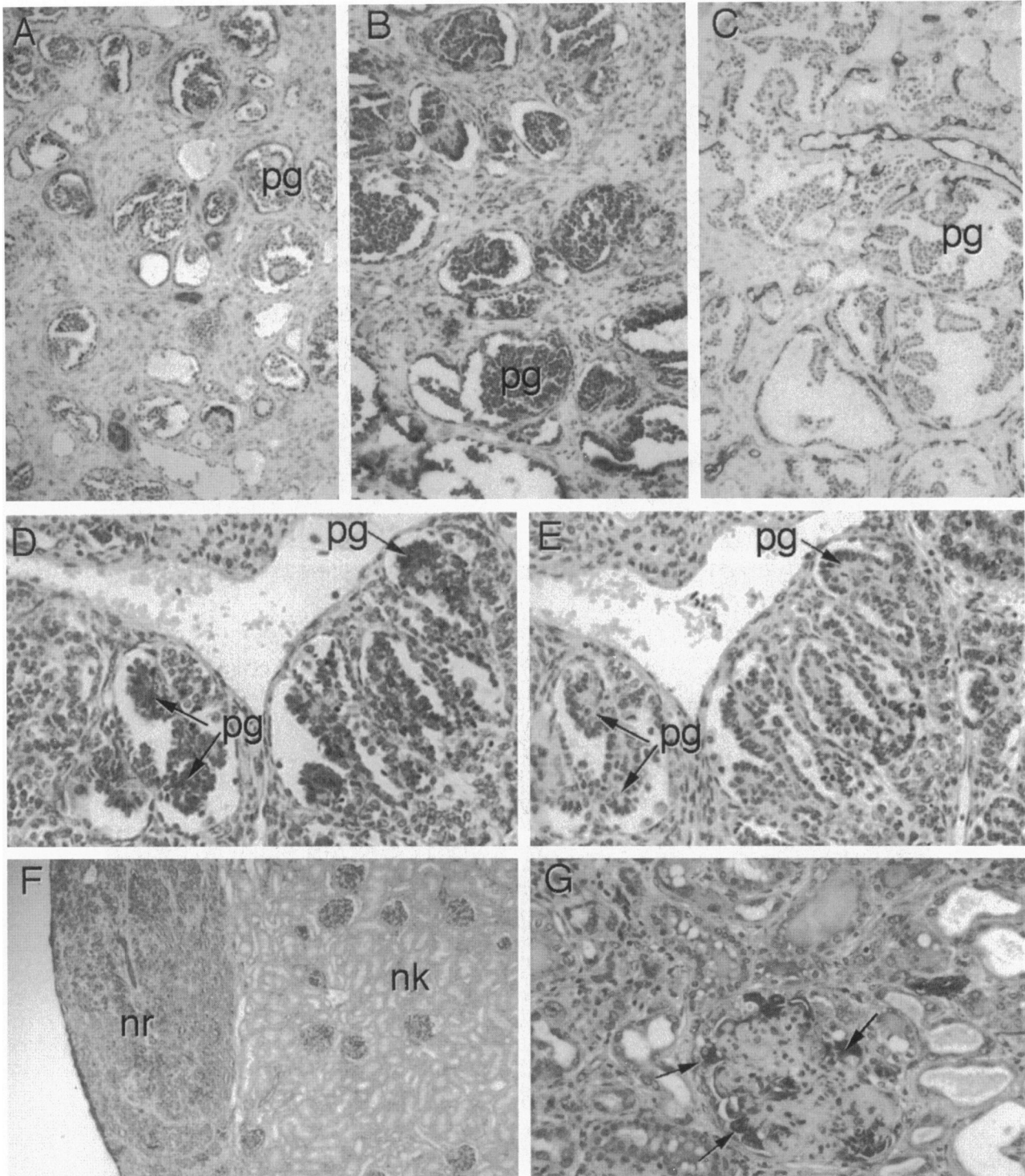
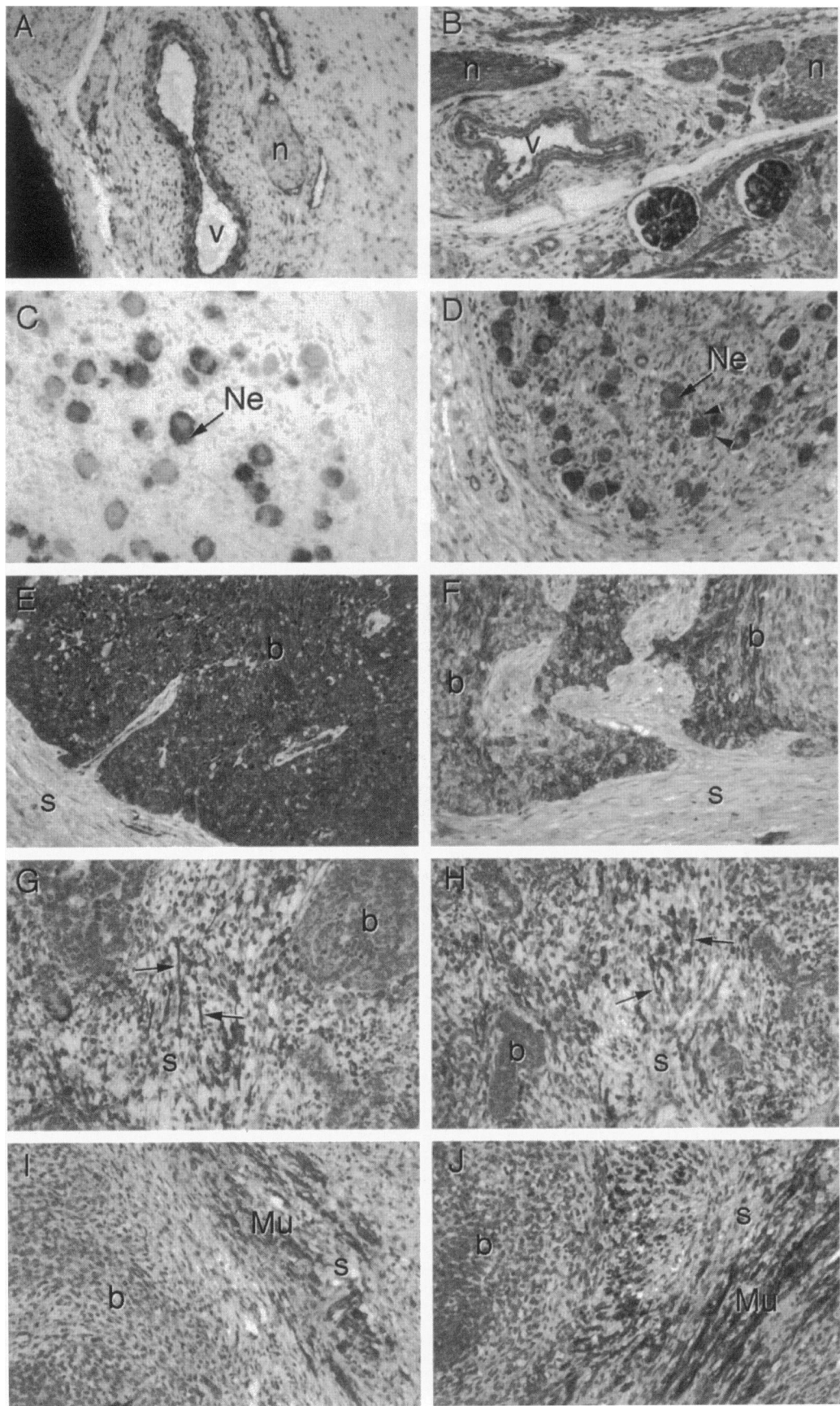


**Figure 4.** Expression of novH mRNA and protein in epithelial component of Wilms' tumors (A to E), nephrogenic rest (F), and Denys-Drash kidney (G. A: *In situ* hybridization using a digoxigenin-labeled antisense novH riboprobe. B, D, F, and G: Immunohistochemistry performed with the K19M antibody preincubated with the K19M-specific peptide. E: Immunohistochemistry performed with the K19M antibody preincubated with the K19M-specific peptide. C: Immunohistochemistry performed with the QBEnd10 antibody, a specific marker of vascular endothelium. A to C: Sections from the pseudoglomeruloid tumor (Wit-75). Note very low level of novH mRNA but high level of novH protein in pseudoglomeruli (pg). Labeling of vascular endothelium of pseudoglomeruli with the QBEnd10 antibody (C) indicated that the novH protein was preferentially associated with pseudoglomerular podocytes. D: Section from the Wit-137 tumor showing novH protein in podocytes of pseudoglomeruli (arrow). E: Adjacent section showing the absence of labeling after peptide competition. F: High levels of novH protein are also detected in pseudoglomeruli of nephrogenic rest (nr) and in well differentiated glomeruli of normal adjacent adult kidney (nk). G: Localization of novH protein in podocytes of sclerotic glomeruli from Denys-Drash kidney (arrows). Magnification  $\times 90$  (all except F) and  $\times 36$  (F).



In conclusion, novH mRNA and protein expression patterns showed an overlap but not a direct correlation. The overall higher expression of novH mRNA in Wilms' tumors, specifically in the blastema, was noted, and accumulation of novH protein in blastema appeared to correlate with co-expression of desmin, a muscle marker. The prevalence of desmin expression without other phenotypic evidence of striated muscle differentiation was also noted. Finally, two distinct patterns of tissue expression were observed: one, as in podocytes and striated muscle, with low to undetectable novH mRNA but high novH protein, and two, as in tubular epithelium, endothelium, and neurons, with nearly comparable levels of novH mRNA and protein. These patterns likely reflect the potentially different functional states of novH.

## Discussion

### *Expression of novH in Developing Kidney and in Wilms' Tumors*

*In situ* hybridization and immunohistochemistry experiments performed on normal human embryonic kidney sections established a good correlation between novH RNA and protein in renal tubules. However, particularly high amounts of novH protein were observed in mature glomerular podocytes in which novH mRNA was barely detectable. These results suggest that the novH protein is stably accumulated in glomerular podocytes undergoing differentiation and that accumulation of novH in these cells that persists after birth likely reflects an important feature of nov biological function(s). The large quantities of novH detected in pseudoglomeruli of both nephrogenic rests and Wilms' tumors, and in hypertrophic podocytes of DDS kidneys, favor novH being required for maintenance of podocyte structure and/or for specific podocytic functions.

Our *in situ* hybridization experiments established that, in the nephrogenic zone where WT1 is highly expressed, novH expression was opposite to that of WT1.<sup>47,48</sup> In addition, novH was also expressed in the ascending portion of the loop of Henle and collecting duct. The apparent lack or barely detectable level of novH mRNA in blastemal cells, which might result from an efficient down-regulation of novH expression by high levels of WT1 in these cells, is in agreement with WT1 acting upstream to novH expression during normal nephrogenesis.<sup>29</sup> In all variants of Wilms' tumors that we have studied, the tumor blastema expressed high but variable levels of novH mRNA. It is worth noting that different histological types of Wilms' tumors also express WT1 protein in this cell compartment (our unpublished results).<sup>47,48</sup> Inasmuch as no clear-cut relationship could

be drawn between the levels of WT1 protein and novH expression, it is possible that the variations of novH expression resulted, at least in part, from individual differences in the ratios of WT1 isoforms. Inefficient post-translational modifications, such as phosphorylations,<sup>49</sup> or a lack of appropriate interactions with other transcriptional regulators, such as p53, par-4,<sup>50-52</sup> and as yet unidentified proteins,<sup>53</sup> could alter WT1 transcriptional activity. Because the zinc finger motif of WT1 has been shown to be involved in interactions with other proteins, such as p53<sup>51</sup> or par-4,<sup>52</sup> the different levels of novH expression observed in the sporadic and DDS tumors that we have analyzed might be related to the nature of the WT1 mutations within the zinc finger domain.

Desmoplastic round-cell tumors have been analyzed for WT1 mutations and found to harbor translocations of WT1, specifically with the EWS gene on chromosome 22.<sup>44-46</sup> The translocation generates an oncogenic fusion protein with the DNA-binding recognition domain of WT1 fused to the transcriptional regulatory domains of EWS. We showed that novH expression was highly expressed in our case of desmoplastic round-cell tumor and that, significantly, there was a comparable high level of desmin expression, also noted by Brodie et al,<sup>46</sup> indicative of muscle commitment as found in other Wilms' tumors. These observations raise the possibility that altered function of WT1 may be sufficient to permit heterotypic muscle differentiation and coordinately the elevated expression of novH.

### *Potential Roles for novH: Secreted versus Intracellular Forms*

Our data showed that the half-life of the intra- and extracellular novH proteins differed. The increased stability of secreted novH protein could result from interactions with other extracellular proteins. The affinity of novH for heparin suggested that it might be stabilized by an interaction with heparan sulfate proteoglycans as previously described for basic fibroblast growth factor.<sup>54</sup> Proteoglycans have been shown to play a crucial role in the morphogenesis of several organs, such as kidney.<sup>55</sup> We also report here that novH is glycosylated. It is well established that glycosylations are involved in a multitude of biological processes, such as protein folding, stability, targeting, and clearance as well as cell-matrix and cell-cell interactions.<sup>56</sup> It is therefore conceivable that the level of novH protein detected in different normal or tumor tissues can be modulated by glycosylations and/or interactions with other proteins and that inefficient post-translational processing of nov or lack of interactions with other cognate proteins in the blastemal cells of Wilms'

**Figure 5.** Expression of novH in nonrenal tissues and in heterotypic tissues of Wilms' tumors. Expression of novH mRNA and protein in sections through 20-week-old fetal kidney (A and B) and normal adult kidney (C and D). A and C: *In situ* hybridization using a digoxigenin-labeled antisense novH riboprobe. B and D: Immunohistochemistry performed with the K19M antibody. Note expression of both mRNA and protein in endothelium of vessels (v) and in the soma of neurons (Ne). The novH protein is present in addition in neuronal processes (D, arrowheads). n, nerve; Ne, neuron; v, vessel. E to J: novH protein (E, G, and I) and desmin (F, H, and J; Dako, clone D33) immunohistochemistry in a case of desmoplastic small round tumor (E and F) and Wilms' tumors (G to J). Note elevated co-expression of novH and desmin both in highly differentiated heterotypic muscle (Mu) and in more mesenchymatous blastema (spindle cells, see arrows in G and H). However, in blastema of the desmoplastic tumor, expression of novH protein was detected in all blastemal components, whereas desmin expression was restricted to a zone closest to the intervening stroma (E and F). b, blastema; s, stroma. Magnification, ×90.

tumors might account for the very low level of novH protein detected in some of the tumors.

### *novH Is Part of a Larger Family of Genes Modulating Growth*

We had previously established<sup>18</sup> that nov is structurally related to immediate-early proteins (CEF10/CYR61 and FISP12/CTGF) reported to stimulate cell proliferation in synergy with growth factors such as TGF- $\beta$  and basic fibroblast growth factor.<sup>21,23</sup> However, several lines of evidence have suggested that nov is involved in negative control of cell growth: 1) the expression of nov was shown to be down-regulated by both oncogenic transformation and serum stimulation whereas it was up-regulated in normal quiescent cells,<sup>28</sup> 2) the expression of a truncated nov was associated with fibroblastic transformation *ex vivo*, and 3) the overexpression of a normal nov led to inhibition of chicken embryo fibroblast growth. It is then tempting to speculate that nov is part of a signaling pathway controlling the establishment and (or) the maintenance of differentiation in various tissues during normal embryogenesis.

The presence of an IGFBP-like domain at the amino terminus of nov raises the possibility that nov is interacting with IGF signaling. Elevated levels of IGF-II have been detected in Wilms' tumors,<sup>57-59</sup> and both expression of IGF-IR and binding of IGF to IGF-IR have been shown to be enhanced in these tumors.<sup>60,61</sup> Also, an increased level of IGF-IR mRNA has been correlated with tumors with heterotypic differentiations.<sup>62</sup> It has recently been shown that the CTGF protein binds IGF-I and IGF-II with low affinities.<sup>40</sup> Although the recombinant novH protein secreted by baculovirus-infected SF9 cells or by the pCMV-novH(S)-transfected MDCK cells did not bind IGF-I and IGF-II in our ligand-binding assays, we cannot exclude the possibility that IGF binding occurs *in vivo*. Alternatively, this domain might be of relevance for a nov-specific biological function independent of IGF. Lack or alteration of the nov-related negative signaling could be among the inappropriate epigenetic signals responsible for abnormal growth and differentiation of embryonic metanephric mesenchymal-derived blastema in Wilms' tumors.

Although the potential of novH for binding and transportation of growth factors remains to be established, if confirmed, it would make novH an important protein for modulating local and distant cellular growth and differentiation functions.

### **Acknowledgments**

We are grateful to Dr. El Naggat and Dr. F. Jaubert for providing, respectively, tissue sections from nephroblastomatosis cases and Denys-Drash-associated tumors. We thank Dr. Leslie Wong, MRC tissue bank, and Dr. John Kingdom for provision of fetal material, and we are grateful to Professor Tony Ridsden and Dr. Pramila Ramani for provision of Wilms' tumors. We thank Sylvia Ko-

cialkowski for her interest and help in early development of studies performed by G. Chevalier in P.N. Schofield's laboratory. Professor John Cowell is thanked for his helpful discussions and access to unpublished data. We also thank Drs. Lalou and Binoux (Hôpital Saint-Antoine, Paris) for performing IGF-binding experiments and M. Starr for assistance with photography.

### **References**

1. Breslow N, Beckwith JB, Ciol M, Sharples K: Age distribution of Wilms' tumor: report from the National Wilms' Tumor Study. *Cancer Res* 1988, 48:1653-1657
2. Breslow NE, Langholz B: Childhood cancer incidence: geographical and temporal variations. *Int J Cancer* 1983, 32:703-716
3. Matsunaga E: Genetics of Wilms' tumor. *Hum Genet* 1981, 57:231-246
4. Beckwith JB, Kiviat NB, Bonadio JF: Nephrogenic rests, nephroblastomatosis, and the pathogenesis of Wilms' tumor. *Pediatr Pathol* 1990, 10:1-36
5. Fearon ER, Vogelstein B, Feinberg AP: Somatic deletion and duplication of genes on chromosome 11 in Wilms' tumours. *Nature* 1984, 309:176-178
6. Haber DA, Buckler AJ, Glaser T, Call KM, Pelletier J, Sohn RL, Douglass EC, Housman DE: An internal deletion within an 11p13 zinc finger gene contributes to the development of Wilms' tumor. *Cell* 1990, 61:1257-1269
7. Koufos A, Hansen MF, Lampkin BC, Workman ML, Copeland NG, Jenkins NA, Cavenee WK: Loss of alleles at loci on human chromosome 11 during genesis of Wilms' tumour. *Nature* 1984, 309:170-172
8. Maw MA, Grundy PE, Millow LJ, Eccles MR, Dunn RS, Smith PJ, Feinberg AP, Law DJ, Paterson MC, Telzerow PE, Call DF, Thompson AD, Richards RI, Reeves AE: A third Wilms' tumor locus on chromosome 16q. *Cancer Res* 1992, 52:3094-3098
9. Newsham I, Kindler-Rohrborn A, Daub D, Cavenee W: A constitutional BWS-related t(11;16) chromosome translocation occurring in the same region of chromosome 16 implicated in Wilms' tumors. *Genes Chromosomes & Cancer* 1995, 12:1-7
10. Orkin SH, Goldman DS, Sallan SE: Development of homozygosity for chromosome 11p markers in Wilms' tumour. *Nature* 1984, 309:172-174
11. Peier AM, Meloni AM, Erling MA, Sandberg AA: Involvement of chromosome 7 in Wilms tumor. *Cancer Genet Cytogenet* 1995, 79:92-94
12. Radice P, Perotti D, De Benedetti V, Mondini P, Radice MT, Pilotti S, Luksch R, Fossati Bellani F, Pierotti MA: Allelotyping in Wilms tumors identifies a putative third tumor suppressor gene on chromosome 11. *Genomics* 1995, 27:497-501
13. Ton CC, Huff V, Call KM, Cohn S, Strong LC, Housman DE, Saunders GF: Smallest region of overlap in Wilms tumor deletions uniquely implicates an 11p13 zinc finger gene as the disease locus. *Genomics* 1991, 10:293-297
14. Pelletier J: Molecular genetics of Wilms' tumor: insights into normal and abnormal renal development. *Can J Oncol* 1994, 4:262-272
15. Hastie ND: The genetics of Wilms' tumor: a case of disrupted development. *Annu Rev Genet* 1994, 28:523-558
16. Chevalier G, Perbal B: Genetic alterations associated with pathologic differentiation of Wilms' tumors. *Bull Cancer* 1997, 84:289-303
17. Perbal B: Contribution of MAV-1-induced nephroblastoma to the study of genes involved in human Wilms' tumor development. *Crit Rev Oncol* 1994, 5:589-613
18. Joliet V, Martinierie C, Dambrine G, Plassiat G, Brisac M, Crochet J, Perbal B: Proviral rearrangements and overexpression of a new cellular gene (nov) in myeloblastosis- associated virus type 1-induced nephroblastomas. *Mol Cell Biol* 1992, 12:10-21
19. Bork P: The modular architecture of a new family of growth regulators related to connective tissue growth factor. *FEBS Lett* 1993, 327:125-130
20. Bradham DM, Igarashi A, Potter RL, Grotendorst GR: Connective tissue growth factor: a cysteine-rich mitogen secreted by human vascular endothelial cells is related to the SRC-induced immediate early gene product CEF-10. *J Cell Biol* 1991, 114:1285-1294

21. Grotendorst GR, Okochi H, Hayashi N: A novel transforming growth factor  $\beta$  response element controls the expression of the connective tissue growth factor gene. *Cell Growth Differ* 1996, 7:469-480
22. Ryseck RP, Macdonald-Bravo H, Mattei MG, Bravo R: Structure, mapping, and expression of fisp-12, a growth factor-inducible gene encoding a secreted cysteine-rich protein. *Cell Growth Differ* 1991, 2:225-233
23. O'Brien TP, Yang GP, Sanders L, Lau LF: Expression of *cyr61*, a growth factor-inducible immediate-early gene. *Mol Cell Biol* 1990, 10:3569-3577
24. O'Brien TP, Lau LF: Expression of the growth factor-inducible immediate early gene *cyr61* correlates with chondrogenesis during mouse embryonic development. *Cell Growth Differ* 1992, 3:645-654
25. Yang GP, Lau LF: *Cyr61*, product of a growth factor-inducible immediate early gene, is associated with the extracellular matrix and the cell surface. *Cell Growth Differ* 1991, 2:351-357
26. Kireeva ML, Mo FE, Yang GP, Lau LF: *Cyr61*, a product of a growth factor-inducible immediate-early gene, promotes cell proliferation, migration, and adhesion. *Mol Cell Biol* 1996, 16:1326-1334
27. Simmons DL, Levy DB, Yannoni Y, Erikson RL: Identification of a phorbol ester-repressible v-src-inducible gene. *Proc Natl Acad Sci USA* 1989, 86:1178-1182
28. Scholz G, Martinerie C, Perbal B, Hanafusa H: Transcriptional down regulation of the nov proto-oncogene in fibroblasts transformed by p60v-src. *Mol Cell Biol* 1996, 16:481-486
29. Martinerie C, Chevalier G, Rauscher F Jr, Perbal B: Regulation of nov by WT1: a potential role for nov in nephrogenesis. *Oncogene* 1996, 12:1479-1492
30. Martinerie C, Huff V, Joubert I, Badzioch M, Saunders G, Strong L, Perbal B: Structural analysis of the human nov proto-oncogene and expression in Wilms tumor. *Oncogene* 1994, 9:2729-2732
31. Yeger H, Cullinane C, Flenniken A, Chilton-MacNeil S, Campbell C, Huang A, Bonetta L, Coppes MJ, Thorner P, Williams BR: Coordinate expression of Wilms' tumor genes correlates with Wilms' tumor phenotypes. *Cell Growth Differ* 1992, 3:855-864
32. Lahoti C, Thorner P, Malkin D, Yeger H: Immunohistochemical detection of p53 in Wilms' tumors correlates with unfavorable outcome. *Am J Pathol* 1996, 148:1577-1589
33. Patwardhan S, Gashler A, Siegel MG, Chang LC, Joseph LJ, Shows TB, Le Beau MM, Sukhatme VP: EGR3, a novel member of the Egr family of genes encoding immediate-early transcription factors. *Oncogene* 1991, 6:917-928
34. Louvard D: Apical membrane aminopeptidase appears at site of cell-cell contact in cultured kidney epithelial cells. *Proc Natl Acad Sci USA* 1980, 77:4132-4136
35. Perbal B: *A Practical Guide to Molecular Cloning*. New York, John Wiley & Sons, 1988
36. Van Regenmortel MH, Briand JP, Muller S, Plaue S: Synthetic polypeptides as antigens. *Laboratory Techniques in Biochemistry and Molecular Biology*. Edited by RH Gurdon, PH Van Kanippenberg. Amsterdam, Elsevier, 1990, pp 95-144
37. Yeger H, Forget D, Alami J, Williams BR: Analysis of WT1 gene expression during mouse nephrogenesis in organ culture. *In Vitro Cell Dev Biol Anim* 1996, 32:496-504
38. Kim H, Yeger H, Han R, Wallace M, Goldstein B, Rotin D: Expression of LAR-PTP2 in rat lung is confined to proliferating epithelia lining the airways and air sacs. *Am J Physiol* 1996, 270:L566-L576
39. Catzavelos C, Bhattacharya N, Ung YC, Wilson JA, Roncari L, Sandhu C, Shaw P, Yeger H, Morava-Protzner I, Kapusta L, Franssen E, Pritchard KI, Slingerland JM: Decreased levels of the cell-cycle inhibitor p27Kip1 protein: prognostic implications in primary breast cancer. *Nature Med* 1997, 3:227-230
40. Kim HS, Nagalla SR, Oh Y, Wilson E, Roberts CT Jr, Rosenfeld RG: Identification of a family of low-affinity insulin-like growth factor binding proteins (IGFBPs): characterization of connective tissue growth factor as a member of the IGFBP superfamily. *Proc Natl Acad Sci USA* 1997, 94:12981-12986
41. Coppes MJ, Liefers GJ, Paul P, Yeger H, Williams BR: Homozygous somatic *Wt1* point mutations in sporadic unilateral Wilms tumor. *Proc Natl Acad Sci USA* 1993, 90:1416-1419
42. Baird PN, Groves N, Haber DA, Housman DE, Cowell JK: Identification of mutations in the WT1 gene in tumours from patients with the WAGR syndrome. *Oncogene* 1992, 7:2141-2149
43. Coppes MJ, Clericuzio CL: Molecular genetic analysis of the WT1 gene in patients suspected to have the Denys-Drash syndrome. *Med Pediatr Oncol* 1994, 23:390
44. Ladanyi M, Gerald W: Fusion of the EWS and WT1 genes in the desmoplastic small round cell tumor. *Cancer Res* 1994, 54:2837-2840
45. Ohno T, Ouchida M, Lee L, Gatalica Z, Rao VN, Reddy ES: The EWS gene, involved in Ewing family of tumors, malignant melanoma of soft parts, and desmoplastic small round cell tumors, codes for an RNA binding protein with novel regulatory domains. *Oncogene* 1994, 9:3087-3097
46. Brodie SG, Stocker SJ, Wardlaw JC, Duncan MH, McConnell TS, Feddersen RM, Williams TM: EWS and WT-1 gene fusion in desmoplastic small round cell tumor of the abdomen. *Hum Pathol* 1995, 26:1370-1374
47. Grubb GR, Yun K, Williams BR, Eccles MR, Reeve AE: Expression of WT1 protein in fetal kidneys and Wilms tumors. *Lab Invest* 1994, 71:472-479
48. Mundlos S, Pelletier J, Darveau A, Bachmann M, Winterpacht A, Zabel B: Nuclear localization of the protein encoded by the Wilms' tumor gene WT1 in embryonic and adult tissues. *Development* 1993, 119:1329-1341
49. Ye Y, Raychaudhuri B, Gurney A, Campbell CE, Williams BR: Regulation of WT1 by phosphorylation: inhibition of DNA binding, alteration of transcriptional activity and cellular translocation. *EMBO J* 1996, 15:5606-5615
50. Maheswaran S, Park S, Bernard A, Morris JF, Rauscher F Jr, Hill DE, Haber DA: Physical and functional interaction between WT1 and p53 proteins. *Proc Natl Acad Sci USA* 1993, 90:5100-5104
51. Maheswaran S, Englert C, Bennett P, Heinrich G, Haber DA: The WT1 gene product stabilizes p53 and inhibits p53-mediated apoptosis. *Genes Dev* 1995, 9:2143-2156
52. Johnstone RW, See RH, Sells SF, Wang J, Muthukumar S, Englert C, Haber DA, Licht JD, Sugrue SP, Roberts T, Rangnekar VM, Shi Y: A novel repressor, par-4, modulates transcription and growth suppression functions of the Wilms' tumor suppressor WT1. *Mol Cell Biol* 1996, 16:6945-6956
53. Wang Z, Qiu Q, Gurrieri M, Huang J, Deuel T: WT1, the Wilms' tumor suppressor gene product, represses transcription through an interactive nuclear protein. *Oncogene* 1995, 10:1243-1247
54. Saksela O, Moscatelli D, Sommer A, Rifkin DB: Endothelial cell-derived heparan sulfate binds basic fibroblast growth factor and protects it from proteolytic degradation. *J Cell Biol* 1988, 107:743-751
55. Bernfield M, Kokenyesi R, Kato M, Hinkes MT, Spring J, Gallo RL, Loe EJ: Biology of the syndecans: a family of transmembrane heparan sulfate proteoglycans. *Annu Rev Cell Biol* 1992, 8:365-393
56. Varki A: Biological roles of oligosaccharides. All of the theories are correct. *Glycobiology* 1993, 3:97-130
57. Reeve AE, Eccles MR, Wilkins RJ, Bell GI, Millow LJ: Expression of insulin-like growth factor-II transcripts in Wilms' tumour. *Nature* 1985, 317:258-260
58. Scott J, Cowell J, Robertson ME, Priestley LM, Wadey R, Hopkins B, Pritchard J, Bell GI, Rall LB, Graham CF, Knott TJ: Insulin-like growth factor-II gene expression in Wilms' tumour and embryonic tissues. *Nature* 1985, 317:260-262
59. Haselbacher GK, Irminger JC, Zapf J, Ziegler WH, Humbel RE: Insulin-like growth factor II in human adrenal pheochromocytomas and Wilms tumors: expression at the mRNA and protein level. *Proc Natl Acad Sci USA* 1987, 84:1104-1106
60. Gansler T, Allen KD, Burant CF, Inabnet T, Scott A, Buse MG, Sens DA, Garvin AJ: Detection of type 1 insulin-like growth factor (IGF) receptors in Wilms' tumors. *Am J Pathol* 1988, 130:431-435
61. Werner H Re, GG, Drummond IA, Sukhatme VP, Rauscher F Jr, Sens DA, Garvin AJ, LeRoith D, Roberts CT Jr: Increased expression of the insulin-like growth factor I receptor gene, IGF1R, in Wilms tumor is correlated with modulation of IGF1R promoter activity by the WT1 Wilms tumor gene product. *Proc Natl Acad Sci USA* 1993, 90:5828-5832
62. Werner H, Rauscher F Jr, Sukhatme VP, Drummond IA, Roberts CT Jr, LeRoith D: Transcriptional repression of the insulin-like growth factor I receptor (IGF-I-R) gene by the tumor suppressor WT1 involves binding to sequences both upstream and downstream of the IGF-I-R gene transcription start site. *J Biol Chem* 1994, 269:12577-12582